Characterization of SARS-CoV-2 replication in human H1299/ACE2 cells: a versatile and practical infection model for antiviral research and beyond

Salgado-Benvindo, C.; Tas, A.; Zevenhoven-Dobbe, J.C.; Meer, Y. van der; Sidorov, I.A.; Leijs, A.A.; ... ; Hemert, M.J. van

Antiviral Research 227 (2024) 105903

Contents lists available at ScienceDirect

Antiviral Research

journal homepage: www.elsevier.com/locate/antiviral

Characterization of SARS-CoV-2 replication in human H1299/ACE2 cells: A versatile and practical infection model for antiviral research and beyond

Clarisse Salgado-Benvindo [a,1], Ali Tas [a,1], Jessika C. Zevenhoven-Dobbe [a,1], Yvonne van der Meer [a], Igor A. Sidorov [a], Anouk A. Leijs [a], Patrick Wanningen [a], Anne T. Gelderloos [b], Puck B. van Kasteren [b], Eric J. Snijder [a,1], Martijn J. van Hemert [a,*,1]

[a] Molecular Virology Laboratory, Center for Infectious Diseases, Leiden University Medical Center, 2333 ZA, Leiden, the Netherlands
[b] Centre for Infectious Disease Control, National Institute for Public Health and the Environment (RIVM), 3720 BA, Bilthoven, the Netherlands

ARTICLE INFO

Keywords:
SARS-CoV-2
Infection model
Lung cells

ABSTRACT

A range of cell culture infection models have been used to study SARS-CoV-2 and perform antiviral drug research. Commonly used African green monkey Vero, human lung-derived Calu-3 and ACE2+TMPRSS2-expressing A549 cells, each have their limitations. Here, we describe human ACE2-expressing H1299 lung cells as a more efficient and robust model for SARS-CoV-2 research. These cells are as easy to handle as Vero cells, support SARS-CoV-2 replication to high titers, display a functional innate immune response and are suitable for plaque assays, microscopy, the production of (genetically stable) virus stocks and antiviral assays. H1299/ACE2-based (CPE reduction) assays can be performed without adding a P-gP drug efflux pump inhibitor, which is often required in Vero-based assays. Moreover, H1299/ACE2 cells allowed us to perform CPE reduction assays with omicron variants that did not work in Vero-based assays. In summary, H1299/ACE2 cells are a versatile infection model to study SARS-CoV-2 replication in the context of antiviral drug development and virus-host interaction studies.

1. Introduction

The Severe Acute Respiratory Syndrome coronavirus 2 virus (SARS-CoV-2) caused a pandemic with unprecedented medical, societal and economic impact. It infected over 700 million people and caused 7 million laboratory-confirmed deaths (as of August 2023). Several efficacious vaccines were developed within a remarkably short time and also antiviral (small molecules, monoclonal antibodies) treatment options became available (Li et al., 2023) and were used in the clinic with varying success for a variety of reasons.

Better antiviral drugs to treat SARS-CoV-2 infection in certain groups of (immune compromised) patients are still needed and development of effective and safe therapeutics with a broad spectrum of activity increases our preparedness for the next emerging coronavirus. Such compounds can be used either prophylactically or post-exposure to treat patients and protect their close contacts. In this manner, antiviral drugs could curb an epidemic at an early stage (Torneri et al., 2020) or slow it down to allow more time for vaccine development and distribution.

Drug development efforts involve the screening and characterization of small molecules in virus-infected cells. For SARS-CoV-2, the cell-based screening of small molecule libraries has relied on a variety of cell lines, each with their own pros and cons. In particular African green monkey kidney Vero or Vero E6 cells (Ammerman et al., 2008) were used frequently, as they support the efficient replication of many viruses and they exhibit a clear cytopathic effect (CPE) that facilitates monitoring of infection and the inhibitory effect of small-molecules. However, Vero cells have a number of disadvantages as they are not human, are unable to produce interferon (IFN) (Desmyter et al., 1968; Emeny and Morgan, 1979), and express high levels of the efflux transporter P-glycoprotein (P-gP), also known as MDR1 (De Rosa et al., 2004), which can lead to an underestimation of compound efficacy. The latter issue can be circumvented by including a P-gP pump inhibitor in antiviral assays (Boras et al., 2021; He et al., 2021) or by using P-gP knockout cells (Zhu et al., 2022).

Another issue with Vero E6 cells is the fast adaptation of SARS-CoV-2, which involves mutations or deletions at or around a multibasic furin

* Corresponding author.
E-mail address: m.j.van_hemert@lumc.nl (M.J. van Hemert).
[1] These authors contributed equally to this work.

https://doi.org/10.1016/j.antiviral.2024.105903
Received 23 January 2024; Received in revised form 12 April 2024; Accepted 6 May 2024
Available online 7 May 2024

cleavage site in the Spike (S) protein. Loss of this cleavage site affects S protein processing, SARS-CoV-2 infectivity, and pathogenesis (Johnson et al., 2021; Peacock et al., 2021), while also causing a pronounced plaque size increase on Vero cells (Ogando et al., 2020) and altering the viral entry pathway, impacting the outcome of antiviral assays.

The use of permissive human cell lines like Calu-3 cells, human adenocarcinoma lung cells isolated from an adult male, can circumvent several of the issues related to the use of Vero cells. However, these cells are more difficult to handle, not very suitable for microscopy, assays using these cells can be less robust and they do not exhibit CPE as clearly as Vero E6 cells (Chu et al., 2020; Park et al., 2021) and therefore cannot be used in CPE reduction assays or plaque assays.

Other human cell lines have also been used in SARS-CoV-2 research, like Caco-2, Caki-1, HEK293T, Huh-7, and engineered A549 cells expressing the angiotensin-converting enzyme 2 (ACE2) receptor, with or without the transmembrane serine protease 2 (TMPRSS2). More complex systems, such as air-liquid interface cultured primary human airway epithelial cells have also been used. Each of these models come with their own limitations, ranging from low susceptibility/progeny titers to culturing difficulties (e.g. slow growth, special and expensive medium requirements) (reviewed in Takayama, 2020).

In this study, we describe the generation, characterization, and application in antiviral assays of H1299/ACE2 cells, human epithelial lung cells isolated from a male patient with carcinoma, which were engineered to ectopically express human ACE2. H1299 cells, with or without overexpression of ACE2, have also been used for certain SARS-CoV-2 experiments by others (Cele et al., 2021, 2022; Chen et al., 2021; Lu et al., 2022), but a more comprehensive and thorough characterization of this infection model, and its description as a tool for antiviral research, has not been published yet.

H1299/ACE2 cells were as easy to handle as Vero E6 cells, supported high levels of SARS-CoV-2 replication, and had a morphology suitable for microscopy. Moreover, we found that these human cells had a functional innate immune response and were easily transfectable. The cells displayed clear CPE upon SARS-CoV-2 infection, even when using omicron isolates (unlike Vero E6). The rapid accumulation of mutations in the SARS-CoV-2 S protein, as typically encountered in Vero E6 cells, was not observed in H1299/ACE2 cells. These features, together with the antiviral assays that we describe here, make H1299/ACE2 cells a versatile infection model for use in antiviral assays and studies on the role of host factors in SARS-CoV-2 replication.

2. Material and methods

2.1. Cell lines

NCl–H1299 cells were kindly provided by Dr. Marc Vooijs (Maastricht University, Maastricht, the Netherlands). Vero E6 and H1299 cells were cultured in Dulbecco's modified Eagle's medium (DMEM, Lonza), with 8% (Vero E6) or 10% (H1299) fetal calf serum (FCS; Bodinco), 100 IU/mL penicillin and 100 μg/mL streptomycin (Sigma-Aldrich). The identity of H1299 and Vero E6 cells was confirmed by STR profiling (100% match). Following pcDNA3-hACE2 transfection (see below), the medium of H1299/ACE2 cells was also supplemented with 1200 μg/mL G418 every third passage.

2.2. Generation and selection of H1299/ACE2 cells

The construction of human ACE2 expression vector pcDNA3-hACE2 was described previously (Broer et al., 2006). H1299 cells were transfected with pcDNA3-hACE2 using Lipofectamine-2000 (ThermoFisher). After 24 h at 37 °C, the transfection medium was replaced with selection medium containing 1200 μg/mL G418. At 4 days post transfection, cells were passaged and culturing was continued in the presence of G418. For enrichment of highly hACE2-expressing cells by fluorescence-activated cell sorting (FACS), cells were first detached using a non-enzymatic cell dissociation solution (Sigma-Aldrich). After washing with PBS containing 0.5% BSA and 2 mM EDTA (FACS buffer), cells were incubated with anti-hACE2 goat antiserum (R&D Systems) for 30 min at 4 °C. Cells were then washed twice with FACS buffer and were incubated with Alexa Fluor 647-conjugated anti-goat secondary antibody (Jackson Immuno) for 30 min at 4 °C. After washing, cells were resuspended in 1 mL FACS buffer and sorted using a BD FACSMelody™ (BD Biosciences) to select the cell population with the highest hACE2 expression. Sorting was repeated once using the same protocol. Sorted cells were resuspended in H1299 medium for further culturing.

2.3. Viruses and infection protocols

SARS-CoV-2 isolate Leiden-0008 (GenBank accession number **MT705206.1**) was isolated at LUMC from a nasopharyngeal sample during the first wave of the pandemic in March 2020. Omicron BA.1 isolate Leiden-O-71084/2021 (GenBank accession number **OR427989.1**) was isolated at LUMC from a clinical sample obtained from the National Institute for Public Health and the Environment (RIVM, Netherlands). Omicron BA.4 and XBB.1.5 were isolated from local clinical samples at LUMC. All virus infections were performed for 1 h at 37 °C in infection medium consisting of Eagle's minimal essential medium (EMEM), 25 mM HEPES (Lonza), 2% FCS, 100 IU/mL penicillin, and 100 μg/mL streptomycin. All experiments with SARS-CoV-2 were performed in biosafety level 3 laboratories at Leiden University Medical Center.

2.4. Plaque assays

Vero E6 and H1299/ACE2 cells were plated 24 h before the assay in 6-well clusters at 3.5×10^6 and 5.0×10^5 cells per well, respectively. Samples were 10-fold serially diluted in infection medium and cells were given a 0.5 mL inoculum for 1 h at 37 °C. After infection, the inoculum was substituted by an overlay of DMEM, 1.2% Avicel, penicillin + streptomycin, 2% FCS, and 50 mM HEPES pH 7.4. After a 3-day incubation, cells were fixed with formaldehyde, and stained with crystal violet to visualize plaques and calculate virus titers.

2.5. RNA isolation and RT-qPCR

Cell culture supernatants were mixed with an equal volume of 3 M guanidine-thiocyanate, 2% N-lauroyl-sarcosine sodium salt, 50 mM Tris-HCl (pH 7.6) and 20 mM EDTA and RNA was isolated via the Bio-on-Magnetic-Beads (BOMB) method (Oberacker et al., 2019), using a Viaflo Assist Plus Robot (Integra) and SpeedBeads magnetic beads (Merck). RT-qPCR to determine absolute viral RNA copy numbers was performed as described previously (Salgado-Benvindo et al., 2020).

Intracellular RNA was isolated using TriPure Isolation Reagent (Sigma-Aldrich). cDNA was generated in a reaction mixture containing 10 U RiboLock RNase Inhibitor (ThermoFisher), 1 mM dNTPs, 200 U RevertAid H minus RT enzyme (ThermoFisher), 1 μg RNA, and 5 ng random hexamers that was incubated at 25 °C for 10 min, 42 °C for 1 h, and 70 °C for 10 min in a thermocycler. cDNA was amplified with primer sets targeting the mRNAs for IFN-β, ISG15, ISG54, Viperin, IL-6, and IL-8 using the iQ™ SYBR® Green Supermix (Bio-Rad) in a CFX384 Touch™ Real-Time PCR Detection System (Bio-Rad). Primer sequences are available on request. Changes in gene expression were calculated through the ΔΔCt method.

2.6. CPE reduction assay

H1299/ACE2 cells (1×10^4 cells/well) were seeded in 96-well clusters. After 24 h, they were given 2-fold serial dilutions of a compound in infection medium and infected with 300 PFU of SARS-CoV-2. After 2 days (or 3 days for the omicron BA.1 variant), cell viability was measured with the CellTiter AQueous MTS Reagent (Promega) to

quantify the antiviral efficacy of compounds. To some assays, 0.25 μM of the P-gP pump inhibitor CP-100356 monohydrochloride (Sigma-Aldrich) was added in addition to the tested compound. This dose of CP-100356 was experimentally determined as optimal (to avoid unwanted effects on the virus or host cell), i.e. the lowest possible dose that had the maximum enhancing effect on the efficacy of remdesivir. Non-infected cells were treated in parallel to determine the compound's cytotoxicity. MTS absorbance was measured with an EnVision multiplate reader (PerkinElmer) at 495 nm and values were normalized to non-infected untreated cells (100%). EC_{50} was determined by non-linear regression using GraphPad Prism.

2.7. Immunofluorescence microscopy

SARS-CoV-2-infected H1299/ACE2 cells grown on glass coverslips were fixed with 3% paraformaldehyde (PFA) in PBS for at least 4 h at room temperature. Coverslips were rinsed with PBS/glycine and permeabilized with 0.2% Triton X-100 for 10 min. Staining was done with the following primary antibodies: anti-hACE2 goat antiserum (R&D Systems); anti-SARS-CoV nsp4 rabbit antiserum (van Hemert et al., 2008); anti-SARS-CoV N protein mouse monoclonal antibody 46–4 (Fang et al., 2006) and anti-SARS-CoV-2 Spike protein human monoclonal antibody P008_052 (Graham et al., 2021) and secondary antibodies: Alexa488-conjugated donkey anti-goat (ThermoFisher); Cy3-donkey-anti-rabbit antibody (Jackson); Cy3-donkey-anti-mouse-IgG (Jackson); Alexa488-goat-anti-human-IgG (ThermoFisher). Nuclei were stained with Hoechst 33,258 (ThermoFisher). After mounting with Prolong Gold (ThermoFisher) coverslips were imaged on a Leica DM6B fluorescence microscope using the LASX software.

2.8. Poly (I:C) transfection

H1299/ACE2 cells were seeded into 12-well clusters at 2×10^5 cells/well. After 24 h, cells were transfected with 500 ng poly (I:C) (Invivogen) using Lipofectamine-2000 (ThermoFisher). After incubation for 7 h at 37 °C, cell lysates were harvested with TriPure Reagent (Sigma-Aldrich) for RNA analysis. At 16 h post-tranfection (hpt), lysates for protein analysis were prepared using 4x Laemmli Sample Buffer.

2.9. Next-generation sequencing (NGS)

SARS-CoV-2 was passaged four times, once every 48 h, on H1299/ACE2 cells (first infection MOI 0.1). Viral RNA was isolated from the medium with TriPure Isolation Reagent (Sigma-Aldrich). After quantification using the Qubit™ RNA High Sensitivity (HS) kit (ThermoFisher), RNA was fragmented by incubation with NEBNext First Strand Synthesis Reaction (New England Labs) and random hexamers for 10 min at 94 °C. NGS was performed by GenomeScan, Leiden, the Netherlands, using a NovaSeq 6000 Sequencing System (Illumina) as described previously (Ogando et al., 2020). After trimming to remove adaptor sequences, sequence reads from SARS-CoV-2 input virus (P0) and the harvest after 4 passages (P4) were mapped to the consensus sequence of the original Wuhan SARS-CoV-2 isolate (GenBank accession number **NC_045512.2**). For analysis of sequence variants, the initial variation frequency threshold was set at 10% to detect newly emerged mutations and variations.

2.10. Immunoblot analysis

H1299/ACE2 cell lysates prepared in 4x Laemmli sample buffer and resolved by SDS-PAGE were blotted onto Hybond 0.2 μM polyvinylidene difluoride membranes (GE Healthcare), which were subsequently blocked with 1% casein in PBS with Tween-20 (PBS-T). Membranes were incubated with anti-ISG15 (Santa Cruz), ISG56 (ThermoFisher), and GAPDH (Cell Signaling Technology), which were detected with secondary and fluorescently labeled tertiary antibodies on an Advanced Q9 Alliance imager (Uvitec Cambridge).

3. Results and discussion

3.1. Generation of the SARS-CoV-2-susceptible H1299/ACE2 cell line

H1299 cells were transfected with a plasmid expressing human ACE2 and the neomycin resistance gene, and selected by culturing in the presence of G418. Cells with high ACE2 expression were selected by two rounds of FACS using an anti-ACE2 antiserum. To assess their susceptibility to infection, H1299/ACE2 cells were infected with SARS-CoV-2 isolate Leiden-0008 at an MOI of 0.1 for 1 h at 37 °C. After 24 h, the culture supernatant was harvested and cells were fixed and analyzed by immunofluorescence microscopy using antibodies recognizing the viral nsp4 protein and human ACE2 (Fig. 1A). Imaging confirmed ACE2 expression and showed that SARS-CoV-2 productively infected H1299/ACE2 cells, leading to CPE and viral spread. The infectious virus titers in supernatant samples from the H1299/ACE2 cells were determined by plaque assays on both H1299/ACE2 and Vero E6 cells, which are commonly used for virus titration. Three-day plaque assays yielded very similar titers on both cell lines (Fig. 1B), confirming that H1299/ACE2 cells are as susceptible to SARS-CoV-2 infection as Vero E6. The plaque size was somewhat more heterogeneous on Vero E6 cells than on H1299/ACE2 cells (Fig. 1C), possibly related to the rapid cell culture adaptation that is known to occur in Vero cells (see 3.3).

As expected, H1299/ACE2 cells could also be infected with SARS-CoV, but not with MERS-CoV (*data not shown*). We speculate that, by introducing other receptors in H1299 cells (such as DPP4, for MERS-CoV), this convenient model could be expanded to other (corona) viruses as well.

3.2. Replication kinetics of SARS-CoV-2 in H1299/ACE2 cells

To investigate SARS-CoV-2 replication kinetics, H1299/ACE2 cells were infected with the early pandemic SARS-CoV-2 isolate Leiden-0008 or with Omicron BA.1 isolate Leiden-O-71084/2021 at an MOI of 0.1 or 1 (titers on Vero E6). Culture supernatants were harvested at 1, 12, 16, 18, 20, 24, and 32 h post-infection (hpi), and also at 40 and 48 hpi for the MOI 0.1 infections, and then subjected to plaque assay on H1299/ACE2 cells (Fig. 2A and B). Both isolates replicated well in these cells, although the omicron isolate showed slower kinetics and replicated to lower titers than the Leiden-0008 isolate.

Infected cells were fixed at 8 hpi and subjected to immunofluorescence staining for viral proteins (S and N) to determine the number of cells initially infected (Fig. 2C). This demonstrated that H1299/ACE2 cells were efficiently infected, especially with the Leiden-0008 variant, which -as expected-at an MOI of 1 caused the infection of ~70% of cells. Infection with the omicron variant appeared somewhat less efficient, as ~33% of the cells were infected at an MOI of 1, instead of the expected 63%. At an MOI of 0.1–7% of the cells were infected. The weaker syncytium formation of the omicron variant compared to Leiden-0008 also contributed to the apparent lower infection efficiency.

These results indicated that both early pandemic and omicron variants of SARS-CoV-2 can efficiently infect H1299/ACE2 cells and that productive replication yields titers comparable to those obtained with Vero E6 cells.

3.3. Genetic stability of SARS-CoV-2 in H1299/ACE2 cells

Rapid cell culture adaptation, associated with mutations in the S gene, is a well-known phenomenon when SARS-CoV-2 is passaged on Vero E6 cells. To investigate the stability of SARS-CoV-2 in H1299/ACE2 cells, we serially passaged the SARS-CoV-2 Leiden-0008 and Leiden-O-71084/2021 isolates in H1299/ACE2 cells and compared the genomic

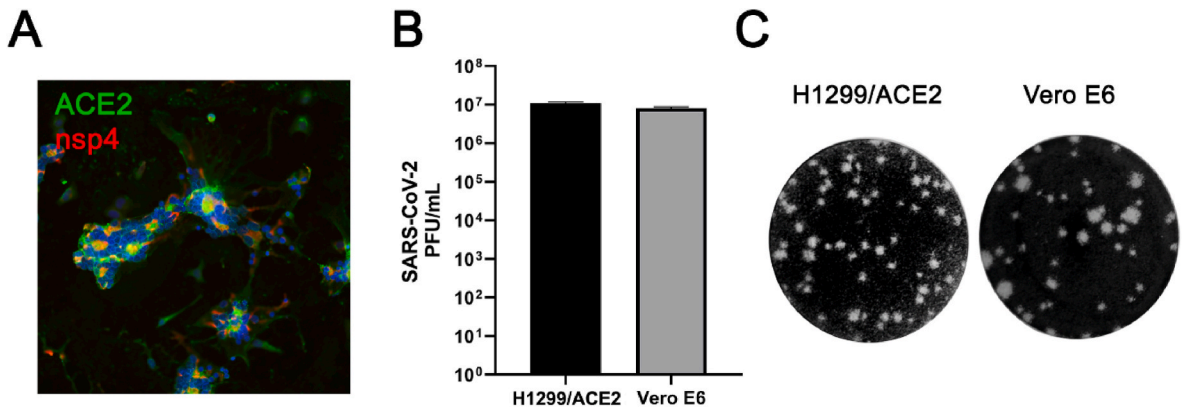

Fig. 1. H1299/ACE2 cells efficiently support SARS-CoV-2 replication. H1299/ACE2 cells were infected with SARS-CoV-2 isolate Leiden-0008 at an MOI of 0.1 and at 24 hpi supernatant was harvested and cells were fixed. (A) Immunofluorescence microscopy of H1299/ACE2 cells stained for human ACE2 and the viral nsp4 protein. The supernatant of H1299/ACE2 cells infected with SARS-CoV-2 Leiden-0008 (MOI 0.1) and harvested at 24 hpi was used in a plaque assay on H1299/ACE2 and Vero E6 cells to compare progeny virus titers (B) and plaque morphology (C).

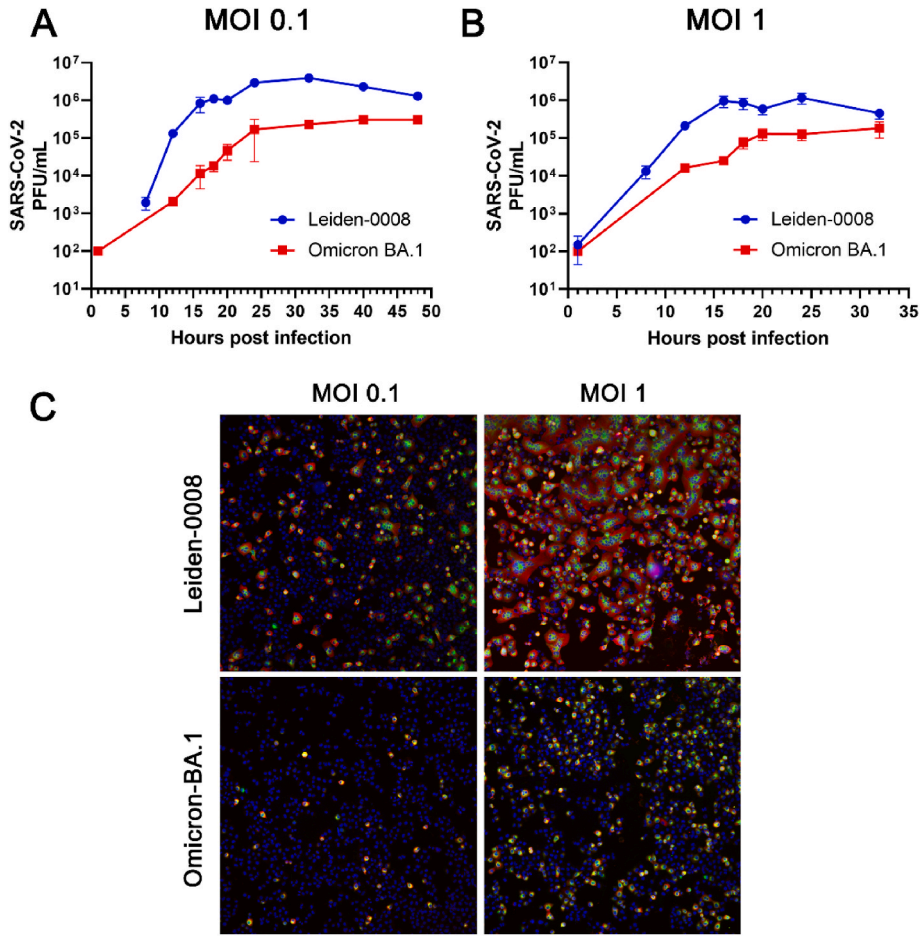

Fig. 2. SARS-CoV-2 replicates to high titers on H1299/ACE2 cells. Cells were infected with SARS-CoV-2 Leiden-0008 or Omicron BA.1 isolate Leiden-O-71084/2021 with an MOI of 0.1 (A) or 1 (B). Supernatant samples of the MOI 0.1 (A) or MOI 1 (B) infections were harvested at different time points and the infectious virus titer was determined by plaque assay on H1299/ACE2 cells. (C) Infected cells on glass coverslips were fixed at 8 hpi and processed for immunofluorescence microscopy to detect the viral N (red) and S (green) proteins.

sequence of the initial virus stock used (P0) with that of the virus harvested after 4 passages (P4). Passaging on Vero E6 cells leads to rapid emergence of variations at or around the furin cleavage site encoding region, usually within a few passages. NGS analysis of the Leiden-0008 strain passaged 4 times on H1299/ACE2 cells indicated that mutations (deletions) that would inactivate the furin cleavage site were only present at a frequency below 5% of the total reads assigned and no mutations were found. No other signs of viral adaptation to H1299/ACE cells were detected by passage 4.

NGS analysis of the Leiden-O-71084/2021 isolate at P0 and P4 did not identify any mutations that became dominant in the quasispecies population at P4. However, the only variation with a frequency above

threshold, i.e. present in 27% of reads at P4, was at nt 23,595, resulting in the R685H substitution in S, which has been shown to inactivate the furin cleavage site (Mykytyn et al., 2021). Whether this variation, which was not observed for Leiden-0008, was merely a chance event or specific adaptation of omicron isolates to H1299/ACE cells requires more extensive analysis. Nevertheless, since at passage 4 the majority (75%) of the omicron viruses did not contain this mutation yet, and since the Wuhan-like Leiden-0008 strain did not change, we still consider H1299/ACE2 cells more useful for virus culture and 'multi-cycle' assays than Vero E6 cells, in which faster adaptation is observed.

To further assess their usefulness, we determined whether H1299/ACE2 cells could be used to recover infectious virus from clinical samples. Recovery attempts of the same 6 clinical specimens on Vero E6, Calu-3 and H1299/ACE cells in parallel, were successful in 5/6, 6/6 and 6/6 cases respectively, highlighting the utility of H1299/ACE2 cells in isolating viruses from clinical samples.

Since H1299/ACE2 cells have low level TMPRSS2 expression, we assume that both the endosomal entry route and TMPRSS2-dependent entry at the plasma membrane are possible in these cells. However, we suspect that mainly the endosomal pathway is used in H1299/ACE2 cells, as we found that hydroxychloroquine, which blocks this entry route had an antiviral effect (EC_{50} ~7 μM), while TMPRSS2 inhibitor camostat had no antiviral effect in H1299/ACE2 cells (EC_{50} > 50 μM). The EC_{50} for hydroxychloroquine in H1299/ACE2 was ~8x times higher than in Vero E6 cells (EC_{50} ~0.8 μM), suggesting that TMPRSS2 might also play a (minor) role in entry. Another indication for functional TMPRSS2 expression on H1299/ACE2 cells is the syncytium formation (not observed in Vero E6) that was observed with early pandemic isolate

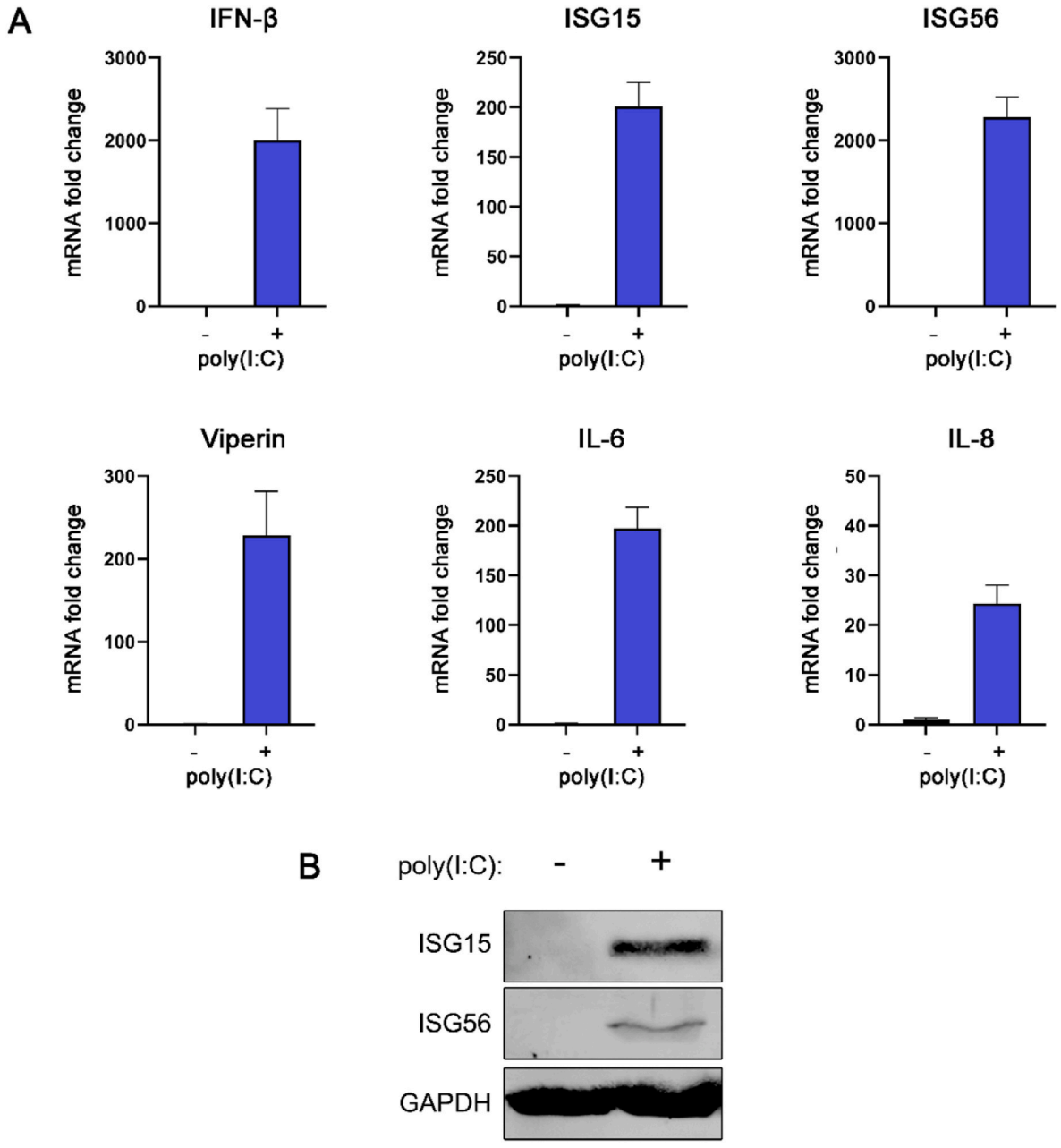

Fig. 3. H1299/ACE2 cells are capable of mounting an innate immune response. H1299/ACE2 cells were transfected with poly (I:C) and cell lysates were harvested for RNA and protein analysis at 7 or 16 hpt, respectively. (A) The relative expression levels of genes involved in the innate immune response and inflammatory response were determined by RT-qPCR. The expression level after poly (I:C) treatment was normalized to that in non-transfected cells. (B) ISG15 and ISG56 proteins in lysates of poly (I:C)-transfected and non-transfected H1299/ACE2 cells were detected by Western blot. GAPDH was used as loading control.

Leiden-0008 (Fig. 2C), for which TMPRSS2 is important (Buchrieser et al., 2020).

3.4. H1299/ACE2 cells are capable of mounting an innate immune response

One of the reasons why Vero E6 cells support the efficient replication of many viruses is that they do not produce interferon, which cripples the innate immune response. To determine if H1299/ACE2 cells are capable of mounting an innate immune response, cells were transfected with poly (I:C) and intracellular RNA was isolated at 7 hpt. The expression of genes involved in the interferon response (IFN-β, ISG15, ISG54 and viperin) and the inflammatory response (IL-6 and IL-8) was compared between poly (I:C)-treated and untreated cells (Fig. 3A). Poly (I:C) transfection led to an increase in the expression of all genes tested, suggesting that H1299/ACE2 cells have a functional innate immune and

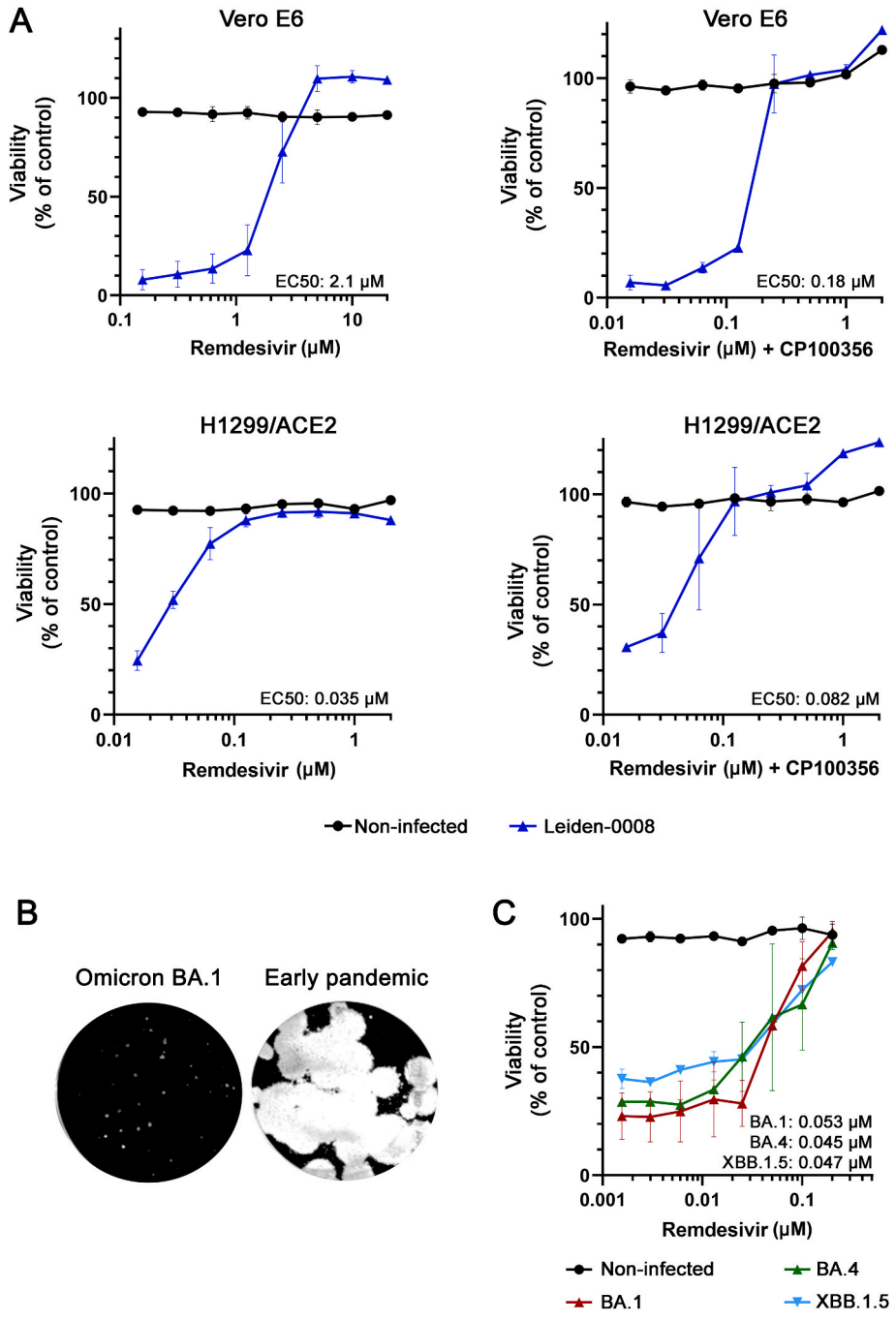

Fig. 4. H1299/ACE2 cells perform well in CPE reduction assays and do not require use of a P-gP pump inhibitor (A) Standard CPE reduction assays done in Vero E6 cells or in H1299/ACE2, in the absence or presence of the P-gP inhibitor CP-100356, using remdesivir as a reference compound. Cells were infected with SARS-CoV-2 early pandemic strain Leiden-0008 at low MOI and, viability was measured with a colorimetric MTS assay, 3 days post infection in the case of Vero E6 or 2 days post infection in the case of H1299/ACE2 cells. (B) Plaque assay with an omicron BA.1 isolate or early pandemic strain Leiden-0008. Fixation and staining were done at 5 days post-infection, instead of the for Leiden-0008 commonly used 3 dpi, to allow appearance of the omicron plaques (C) CPE reduction assay with omicron strains BA.1, BA.4 and XBB.1.5, with viability determination at 3 days post infection. In all experiments, viability of non-infected cells treated with remdesivir was determined in parallel to assess possible cytotoxic effects. Viability was normalized to that of non-infected, untreated cells (100%). Mean ± SEM of 2 independent experiments performed in quadruplicate are shown.

inflammatory response. Western blot analysis of lysates harvested at 16 hpt confirmed that not only at transcription level, but also at the protein level, these cells displayed a functional innate immune response, as a clear increase in ISG15 and ISG56 protein levels was observed after poly (I:C) treatment (Fig. 3B). Besides the fact that they are human cells, their capability of generating a functional innate immune response makes H1299/ACE2 a more relevant infection model for studying virus-host interactions than Vero E6 cells.

3.5. H1299/ACE2 cells are suitable for testing antiviral compounds

To determine if H1299/ACE2 cells can be used in antiviral drug screening assays, we developed a CPE reduction assay with SARS-CoV-2 Leiden-0008. In our standard Vero E6 cell-based CPE reduction assays, remdesivir is often used as reference compound, which on average yielded an EC_{50} value of ~0.18 μM in the presence of the P-gP efflux pump inhibitor CP-100356 (Fig. 4A). In the absence of the P-gP efflux pump inhibitor, the EC_{50} value for remdesivir increased to an average value of 2.1 μM in Vero cells. The efflux of (potential) inhibitors that requires the use of CP-100356, as has also been described by several other research groups (Boras et al., 2021; He et al., 2021), represents a disadvantage of the application of Vero E6 cells in antiviral assays. To assess whether the P-gP efflux pump also poses a problem in H1299/ACE2 cells, we determined the EC_{50} for remdesivir in the presence and absence of CP-100356 (Fig. 4A). Remdesivir inhibited SARS-CoV-2 replication with an EC_{50} of approximately ~0.035 μM in the absence of CP-100356 and 0.082 μM in the presence of the P-gP inhibitor (Fig. 4A), suggesting that this drug efflux pump is not present or at least not affecting the intracellular concentration of antiviral compounds. The fact that CP-100356 can be omitted in screening assays is another advantage of H1299/ACE2 cells over Vero E6 cells, since this compound could interact with compounds being screened.

The CPE of omicron isolates on Vero E6 cells is less pronounced than that of earlier variants and therefore it was not possible - at least in our hands - to perform CPE reduction assays with these variants in our Vero cell-based assays. For example, after a 3-day CPE reduction assay with omicron in Vero E6 cells, 98.5% of cells remained viable, while this was around 20% when earlier variants were used. The tiny plaques - compared to those of the early pandemic isolate – that are visible in the 5-day plaque assay in Fig. 4B indicate that omicron isolates replicated in our Vero E6 cells, but the limited CPE did not allow us to develop CPE reduction assays in these cells.

The use of H1299/ACE2 cells allowed us to solve this problem, as we were able to develop functional CPE reduction assays with different omicron isolates, which caused sufficient CPE, with generally ~20–30% viability remaining (Fig. 4C). For the omicron isolates, the ~50 nM EC_{50} value of remdesivir is similar to the value found for the early pandemic Leiden-0008 isolate (~35 nM).

4. Conclusion

Our newly generated human H1299/ACE2 lung cell line is highly susceptible to SARS-CoV-2, and characterization of virus replication demonstrated its suitability for antiviral assays and studying host responses. H1299/ACE2 cells can be cultured as easily as Vero E6 cells, have a morphology suitable for microscopy, and exhibited CPE upon infection with SARS-CoV-2, including omicron variants. These cells could be infected as efficiently as Vero E6 cells, supported virus replication to high titers and kinetics comparable to Vero E6. However, H1299/ACE2 cells have several advantages over Vero E6 cells. 1) H1299/ACE2 cells are human lung cells, thereby more relevant and which also means that more (functional genetic) research tools are available. 2) Unlike Vero cells, H1299/ACE2 cells are capable of mounting a functional innate immune response, making them more relevant for virus-host interaction studies. 3) SARS-CoV-2 was genetically more stable on H1299/ACE2 cells, which is beneficial for multi-cycle antiviral assays and growing virus stocks. 4) Robust CPE reduction assays with H1299/ACE2 cells yielded similar EC_{50} values for remdesivir as Vero-based assays, but without the need for a P-gP pump inhibitor. 5) Unlike Vero E6 cells, H1299/ACE2 cells can be used in CPE reduction assays with omicron variants, which allows comparison and spectrum of activity determination with a wider range of virus isolates.

Taken together, our characterization of SARS-CoV-2 replication in H1299/ACE2 cells and the antiviral assays described here provide a useful addition to the arsenal of tools to study SARS-CoV-2 and identify inhibitors of replication.

CRediT authorship contribution statement

Clarisse Salgado-Benvindo: Writing – review & editing, Writing – original draft, Visualization, Project administration, Methodology, Investigation, Funding acquisition, Formal analysis, Data curation. **Ali Tas:** Writing – review & editing, Visualization, Validation, Methodology, Investigation, Formal analysis. **Jessika C. Zevenhoven-Dobbe:** Writing – review & editing, Visualization, Methodology, Investigation, Formal analysis. **Yvonne van der Meer:** Methodology, Investigation, Formal analysis, Data curation. **Igor A. Sidorov:** Writing – review & editing, Methodology, Formal analysis. **Anouk A. Leijs:** Methodology. **Patrick Wanningen:** Investigation. **Anne T. Gelderloos:** Methodology. **Puck B. van Kasteren:** Writing – review & editing, Methodology. **Eric J. Snijder:** Writing – review & editing, Writing – original draft, Supervision, Resources, Project administration, Funding acquisition, Formal analysis, Conceptualization. **Martijn J. van Hemert:** Writing – review & editing, Writing – original draft, Visualization, Validation, Supervision, Resources, Project administration, Funding acquisition, Formal analysis, Conceptualization.

Declaration of competing interest

The authors declare that they have no known competing financial interests or personal relationships that could have appeared to influence the work reported in this paper.

Data availability

Data will be made available on request.

Acknowledgments

We thank Marc Vooijs from Maastricht University (the Netherlands) for providing the NCl–H1299 parental cell line and Ying Fang and Kathie Doores for providing antibodies. We thank Emmely Treffers for technical assistance. Clarisse Salgado-Benvindo was supported by the Coordination for the Improvement of Higher Education Personnel (CAPES, process number 88881.171440/2018–01), Ministry of Education, Brazil.

This work was supported in part by the Corona Accelerated R&D in Europe (CARE) project funded by the Innovative Medicines Initiative two Joint Undertaking (JU) under grant agreement no. 101005077.

References

Ammerman, N.C., Beier-Sexton, M., Azad, A.F., 2008. Growth and maintenance of Vero cell lines. Curr. Protoc. Microbiol. Appendix. 4. Appendix 4E.

Boras, B., Jones, R.M., Anson, B.J., Arenson, D., Aschenbrenner, L., Bakowski, M.A., Beutler, N., Binder, J., Chen, E., Eng, H., Hammond, H., Hammond, J., Haupt, R.E., Hoffman, R., Kadar, E.P., Kania, R., Kimoto, E., Kirkpatrick, M.G., Lanyon, L., Lendy, E.K., Lillis, J.R., Logue, J., Luthra, S.A., Ma, C., Mason, S.W., McGrath, M.E., Noell, S., Obach, R.S., Mn, O.B., O'Connor, R., Ogilvie, K., Owen, D., Pettersson, M., Reese, M.R., Rogers, T.F., Rosales, R., Rossulek, M.I., Sathish, J.G., Shirai, N., Steppan, C., Ticehurst, M., Updyke, L.W., Weston, S., Zhu, Y., White, K.M., Garcia-Sastre, A., Wang, J., Chatterjee, A.K., Mesecar, A.D., Frieman, M.B., Anderson, A.S., Allerton, C., 2021. Preclinical characterization of an intravenous coronavirus 3CL protease inhibitor for the potential treatment of COVID19. Nat. Commun. 12, 6055.

Broer, R., Boson, B., Spaan, W., Cosset, F.L., Corver, J., 2006. Important role for the transmembrane domain of severe acute respiratory syndrome coronavirus spike protein during entry. J. Virol. 80, 1302–1310.
Buchrieser, J., Dufloo, J., Hubert, M., Monel, B., Planas, D., Rajah, M.M., Planchais, C., Porrot, F., Guivel-Benhassine, F., Van der Werf, S., Casartelli, N., Mouquet, H., Bruel, T., Schwartz, O., 2020. Syncytia formation by SARS-CoV-2-infected cells. EMBO J. 39, e106267.
Cele, S., Gazy, I., Jackson, L., Hwa, S.H., Tegally, H., Lustig, G., Giandhari, J., Pillay, S., Wilkinson, E., Naidoo, Y., Karim, F., Ganga, Y., Khan, K., Bernstein, M., Balazs, A.B., Gosnell, B.I., Hanekom, W., Moosa, M.S., Lessells, R.J., de Oliveira, T., Sigal, A., Network for Genomic Surveillance in SouthA., Team, C.-K, 2021. Escape of SARS-CoV-2 501Y.V2 from neutralization by convalescent plasma. Nature 593, 142–146.
Cele, S., Jackson, L., Khoury, D.S., Khan, K., Moyo-Gwete, T., Tegally, H., San, J.E., Cromer, D., Scheepers, C., Amoako, D.G., Karim, F., Bernstein, M., Lustig, G., Archary, D., Smith, M., Ganga, Y., Jule, Z., Reedoy, K., Hwa, S.H., Giandhari, J., Blackburn, J.M., Gosnell, B.I., Abdool Karim, S.S., Hanekom, W., Ngs, S.A., Team, C.-K., von Gottberg, A., Bhiman, J.N., Lessells, R.J., Moosa, M.S., Davenport, M.P., de Oliveira, T., Moore, P.L., Sigal, A., 2022. Omicron extensively but incompletely escapes Pfizer BNT162b2 neutralization. Nature 602, 654–656.
Chen, J., Fan, J., Chen, Z., Zhang, M., Peng, H., Liu, J., Ding, L., Liu, M., Zhao, C., Zhao, P., Zhang, S., Zhang, X., Xu, J., 2021. Nonmuscle myosin heavy chain IIA facilitates SARS-CoV-2 infection in human pulmonary cells. Proc. Natl. Acad. Sci. U. S. A. 118.
Chu, H., Chan, J.F., Yuen, T.T., Shuai, H., Yuan, S., Wang, Y., Hu, B., Yip, C.C., Tsang, J. O., Huang, X., Chai, Y., Yang, D., Hou, Y., Chik, K.K., Zhang, X., Fung, A.Y., Tsoi, H. W., Cai, J.P., Chan, W.M., Ip, J.D., Chu, A.W., Zhou, J., Lung, D.C., Kok, K.H., To, K. K., Tsang, O.T., Chan, K.H., Yuen, K.Y., 2020. Comparative tropism, replication kinetics, and cell damage profiling of SARS-CoV-2 and SARS-CoV with implications for clinical manifestations, transmissibility, and laboratory studies of COVID-19: an observational study. Lancet Microbe 1, e14–e23.
De Rosa, M.F., Sillence, D., Ackerley, C., Lingwood, C., 2004. Role of multiple drug resistance protein 1 in neutral but not acidic glycosphingolipid biosynthesis. J. Biol. Chem. 279, 7867–7876.
Desmyter, J., Melnick, J.L., Rawls, W.E., 1968. Defectiveness of interferon production and of rubella virus interference in a line of African green monkey kidney cells (Vero). J. Virol. 2, 955–961.
Emeny, J.M., Morgan, M.J., 1979. Regulation of the interferon system: evidence that Vero cells have a genetic defect in interferon production. J. Gen. Virol. 43, 247–252.
Fang, Y., Pekosz, A., Haynes, L., Nelson, E.A., Rowland, R.R., 2006. Production and characterization of monoclonal antibodies against the nucleocapsid protein of SARS-CoV. Adv. Exp. Med. Biol. 581, 153–156.
Graham, C., Seow, J., Huettner, I., Khan, H., Kouphou, N., Acors, S., Winstone, H., Pickering, S., Galao, R.P., Dupont, L., Lista, M.J., Jimenez-Guardeno, J.M., Laing, A. G., Wu, Y., Joseph, M., Muir, L., van Gils, M.J., Ng, W.M., Duyvesteyn, H.M.E., Zhao, Y., Bowden, T.A., Shankar-Hari, M., Rosa, A., Cherepanov, P., McCoy, L.E., Hayday, A.C., Neil, S.J.D., Malim, M.H., Doores, K.J., 2021. Neutralization potency of monoclonal antibodies recognizing dominant and subdominant epitopes on SARS-CoV-2 Spike is impacted by the B.1.1.7 variant. Immunity 54, 1276–1289 e1276.
He, X., Quan, S., Xu, M., Rodriguez, S., Goh, S.L., Wei, J., Fridman, A., Koeplinger, K.A., Carroll, S.S., Grobler, J.A., Espeseth, A.S., Olsen, D.B., Hazuda, D.J., Wang, D., 2021. Generation of SARS-CoV-2 reporter replicon for high-throughput antiviral screening and testing. Proc. Natl. Acad. Sci. U. S. A. 118.
Johnson, B.A., Xie, X., Bailey, A.L., Kalveram, B., Lokugamage, K.G., Muruato, A., Zou, J., Zhang, X., Juelich, T., Smith, J.K., Zhang, L., Bopp, N., Schindewolf, C., Vu, M., Vanderheiden, A., Winkler, E.S., Swetnam, D., Plante, J.A., Aguilar, P., Plante, K.S., Popov, V., Lee, B., Weaver, S.C., Suthar, M.S., Routh, A.L., Ren, P., Ku, Z., An, Z., Debbink, K., Diamond, M.S., Shi, P.Y., Freiberg, A.N., Menachery, V. D., 2021. Loss of furin cleavage site attenuates SARS-CoV-2 pathogenesis. Nature 591, 293–299.
Li, G., Hilgenfeld, R., Whitley, R., De Clercq, E., 2023. Therapeutic strategies for COVID-19: progress and lessons learned. Nat. Rev. Drug Discov. 22, 449–475.
Lu, Y., Zhu, Q., Fox, D.M., Gao, C., Stanley, S.A., Luo, K., 2022. SARS-CoV-2 down-regulates ACE2 through lysosomal degradation. Mol. Biol. Cell 33, ar147.
Mykytyn, A.Z., Breugem, T.I., Riesebosch, S., Schipper, D., van den Doel, P.B., Rottier, R. J., Lamers, M.M., Haagmans, B.L., 2021. SARS-CoV-2 entry into human airway organoids is serine protease-mediated and facilitated by the multibasic cleavage site. Elife 10.
Oberacker, P., Stepper, P., Bond, D.M., Hohn, S., Focken, J., Meyer, V., Schelle, L., Sugrue, V.J., Jeunen, G.J., Moser, T., Hore, S.R., von Meyenn, F., Hipp, K., Hore, T. A., Jurkowski, T.P., 2019. Bio-On-Magnetic-Beads (BOMB): open platform for high-throughput nucleic acid extraction and manipulation. PLoS Biol. 17, e3000107.
Ogando, N.S., Dalebout, T.J., Zevenhoven-Dobbe, J.C., Limpens, R., van der Meer, Y., Caly, L., Druce, J., de Vries, J.J.C., Kikkert, M., Barcena, M., Sidorov, I., Snijder, E.J., 2020. SARS-coronavirus-2 replication in Vero E6 cells: replication kinetics, rapid adaptation and cytopathology. J. Gen. Virol. 101, 925–940.
Park, B.K., Kim, D., Park, S., Maharjan, S., Kim, J., Choi, J.K., Akauliya, M., Lee, Y., Kwon, H.J., 2021. Differential signaling and virus production in calu-3 cells and Vero cells upon SARS-CoV-2 infection. Biomol Ther. (Seoul) 29, 273–281.
Peacock, T.P., Goldhill, D.H., Zhou, J., Baillon, L., Frise, R., Swann, O.C., Kugathasan, R., Penn, R., Brown, J.C., Sanchez-David, R.Y., Braga, L., Williamson, M.K., Hassard, J. A., Staller, E., Hanley, B., Osborn, M., Giacca, M., Davidson, A.D., Matthews, D.A., Barclay, W.S., 2021. The furin cleavage site in the SARS-CoV-2 spike protein is required for transmission in ferrets. Nat. Microbiol. 6, 899–909.
Salgado-Benvindo, C., Thaler, M., Tas, A., Ogando, N.S., Bredenbeek, P.J., Ninaber, D.K., Wang, Y., Hiemstra, P.S., Snijder, E.J., van Hemert, M.J., 2020. Suramin inhibits SARS-CoV-2 infection in cell culture by interfering with early steps of the replication cycle. Antimicrob. Agents Chemother. 64.
Takayama, K., 2020. In vitro and animal models for SARS-CoV-2 research. Trends Pharmacol. Sci. 41, 513–517.
Torneri, A., Libin, P., Vanderlocht, J., Vandamme, A.M., Neyts, J., Hens, N., 2020. A prospect on the use of antiviral drugs to control local outbreaks of COVID-19. BMC Med. 18, 191.
van Hemert, M.J., van den Worm, S.H., Knoops, K., Mommaas, A.M., Gorbalenya, A.E., Snijder, E.J., 2008. SARS-coronavirus replication/transcription complexes are membrane-protected and need a host factor for activity in vitro. PLoS Pathog. 4, e1000054.
Zhu, Y., Binder, J., Yurgelonis, I., Rai, D.K., Lazarro, S., Costales, C., Kobylarz, K., McMonagle, P., Steppan, C.M., Aschenbrenner, L., Anderson, A.S., Cardin, R.D., 2022. Generation of a VeroE6 Pgp gene knock out cell line and its use in SARS-CoV-2 antiviral study. Antivir. Res. 208, 105429.